Supplemantary Information

Self-organization of rod–coil *tri*- and *tetra*-arm star metallo-supramolecular block copolymers in selective solvents

Jean-François Gohy, Manuela Chiper, Pierre Guillet, Charles-André Fustin, Stephanie Hoeppener, Andreas Winter, Richard Hoogenboom, Ulrich S. Schubert

1. Characterization of the three fractions obtained after synthesis of the tri-arm star metallo supramolecular block copolymer

Purification of the crude reaction product was performed by repetitive fractionation by preparative size exclusion chromatography (BioBeads S-X1 in acetone). Three fractions, namely $\mathbf{5F_1}$, $\mathbf{5F_2}$ and $\mathbf{5F_3}$ were collected. These fractions were firstly checked by SEC with a RI detector aiming for a higher and monomodal molar mass distribution of the desired *tri*-arm star metallo supramolecular block copolymer in comparison to the starting material **2** and the model complex **3**. Fraction $\mathbf{5F_1}$ displayed the highest molar mass from the analyzed fractions (Figure 3 in the paper). This feature could be attributed to the full complexation of all the three terpyridines of **4** with PEG arms **2**. Following the same reasoning, fraction $\mathbf{5F_2}$ might be attributed to **4** complexed with two PEG arms and $\mathbf{5F_3}$ might be represented by **4** complexed with one PEG arm. However, it should be noted that the used PEG had a defined molar mass distribution and, thus, the observed differences in molar mass might be related to the molar mass of the attached PEG chains. Furthermore, SEC with an in-line diode array detector proved the existence and the stability of *bis*-2,2':6',2"-terpyridine-Ru(II) connectivity from the analyzed fractions $\mathbf{5F_1}$-$\mathbf{F_3}$ as revealed by the monomodal distribution of the M_n correlated with the UV-Vis absorption around 500 nm. The molar mass of the fractions could not be calculated from SEC since the analyzed structures contain multiple charges and their hydrodynamic volume (tri-star) is very different compared to the neutral linear polymers used for SEC calibrations. Therefore, from SEC results no definitive conclusions regarding *mono*-, *di*- or *tri*-functionalization of **4** could be drawn.

^{1}H-NMR spectra of the studied fractions **5F$_1$-F$_3$** showed in all cases the same type of shifts for the aromatic protons (compared to **4**), which proved the formation of *bis*-2,2':6',2"-terpyridine-Ru(II) connectivity between the two terpyridine groups of **2** and **4**, respectively. Two dimensional ^{1}H-^{1}H COSY NMR was used for the assignment of the complexed terpyridine protons *via* the cross-peaks. No uncomplexed signals could be observed in the terpyridine region of **5F$_1$-F$_3$**, which indicate that full complexation occurred in all three fractions: **5F$_1$**, **5F$_2$** and **5F$_3$** respectively. Moreover, full complexation was further confirmed for **5F$_1$** by addition of Fe(II) acetate that did not result in the characteristic *bis*-2,2':6',2"-terpyridine-Fe(II) MLCT band at 590 nm. Furthermore, the CH_2 signals of the PEG backbone and the signals belonging to the alkyl groups of the core could be distinguished. In order to determine the degree of complexation for the isolated fractions **5F$_1$-F$_3$**, the integrals of the terpyridine protons and CH_2- (situated next to the PEG polymer backbone) were compared demonstrating that **5F$_1$** was fully complexed while **5F$_2$** and **5F$_3$** revealed a lower integral for the PEG signal indicating partially complexation of the three arm star **4**. These opposite results revealed that all present terpyridines are complexed but not all terpyridines still bear the PEG chain.

The **5F$_1$-F$_3$** fractions were also investigated by UV-Vis absorption spectroscopy (Figure S1). In order to allow a clear comparison between the uncomplexed and Ru(II) complexed species, Figure S1 also displays the absorption of **4**. All absorption spectra showed characteristic bands for the terpyridine moiety at 280 nm. The uncomplexed **4** exhibited a strong absorption at 400 nm which is assigned to the π-π* transition from the conjugated spacer decorated by the terpyridine units. **5F$_1$-F$_3$** showed MLCT bands around 500 nm corresponding to the typical absorption of the *bis*-2,2':6',2"-terpyridine-Ru(II) complexes. Moreover, the formation of the *bis*-2,2':6',2"-terpyridine-Ru(II) connectivity in **5F$_1$-F$_3$** is proven by the considerably decreased intensity of the π-π* transition belonging to the conjugated spacer due to quenching by the *bis*-2,2':6',2"-terpyridine-Ru(II) complex. On the other hand, fraction **5F$_3$** revealed weaker absorption bands in comparison to **5F$_1$** and **5F$_2$**, which indicated that indeed **5F$_3$** contained a lower quantity of *bis*-2,2':6',2"-terpyridine-Ru(II) complexes (due to incomplete complexation of the terpyridine moieties of ligand **4**).

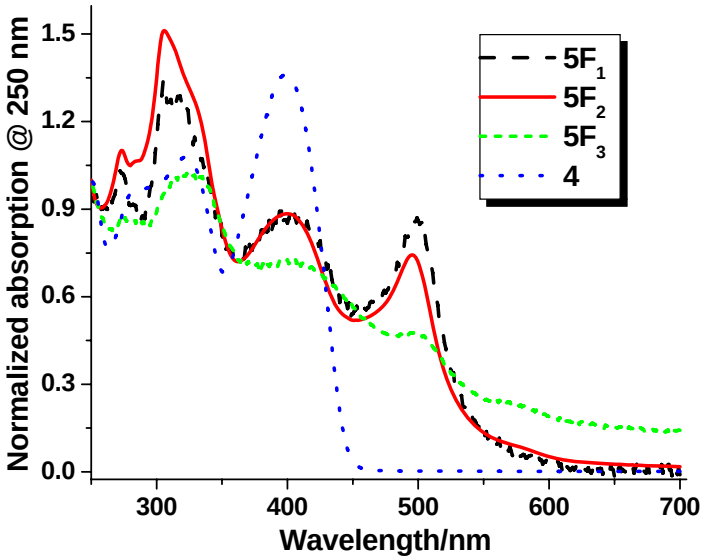

Figure S1: Comparison of the normalized absorption spectra of **4** and **5F$_1$-F$_3$**. All spectra were recorded at a concentration of 10^{-5} M in CH_2Cl_2 (**4**) and CH_3CN (**5**), respectively.

2. Characterization of the tetra-arm star metallo supramolecular block copolymer

The tetra-arm star metallo supramolecular block copolymer **7** is characterized by a monomodal distribution of higher molar mass in comparison to its precursor **2** and the model complex **3** (Figure 4 in the paper). Nevertheless, **7** displays a small shoulder at lower elution time that might correspond to minor impurities such as, *e.g.*, the model complex **3** or defect structures. Repetitions of the SEC analysis revealed always the same distribution of the SEC curve. Moreover, the molar mass of **7** could not be calculated from SEC since the analyzed structure had incorporated many charges and had a very different hydrodynamic volume than the neutral linear polymers used for SEC calibrations. Moreover, SEC with an in-line diode array detector proved that the synthesized structure **7** is stable during the SEC measurement as demonstrated by a monomodal molar mass distribution together with the UV-Vis absorption around 500 nm.

The ^{1}H-NMR spectrum of **7** revealed clear shifts of the terpyridine protons in comparison to **2** and **6**. The proton assignments were performed *via* the cross-peaks of the 2-dimensional ^{1}H-^{1}H-COSY NMR which proved the formation of the *bis*-2,2':6',2''-terpyridine-Ru(II) connectivity between the starting materials **2** and **6**.

The isolated fraction of **7** was investigated by UV-Vis absorption spectroscopy (Figure S2) in comparison to the uncomplexed **6** bearing a conjugated rigid rod core spacer. Both absorption spectra displayed the characteristic bands for the terpyridine moiety: 290 nm in the case of the uncomplexed **6** and 307 nm for **7** which proved the formation of *bis*-2,2':6',2"-terpyridine-Ru(II) complexes. Following the same behavior as **5**, the uncomplexed **6** exhibited a strong absorption at 410 nm which belongs to the π-π* transition from the conjugated spacer between the terpyridine units. **7** showed a characteristic MLCT band around 498 nm that corresponded to the typical absorption of the octahedral *bis*-2,2':6',2"-terpyridine-Ru(II) complexes. Moreover, **7** also displayed a considerable decreased intensity of the π-π* transition belonging to the conjugated spacer.

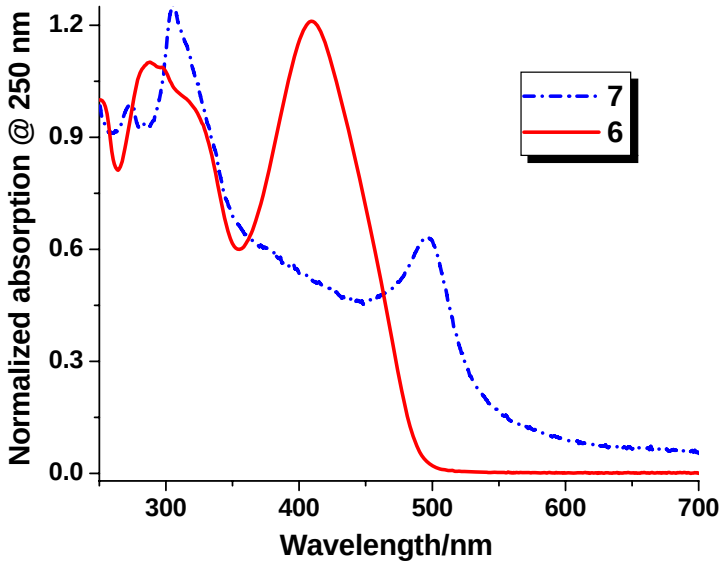

Figure S2: Comparison of the normalized absorption spectra of **6** and **7**. The spectra were recorded at a concentration of 10^{-5} M in CH_2Cl_2 (**6**) or CH_3CN (**7**), respectively.

3. Additional cryo-TEM pictures

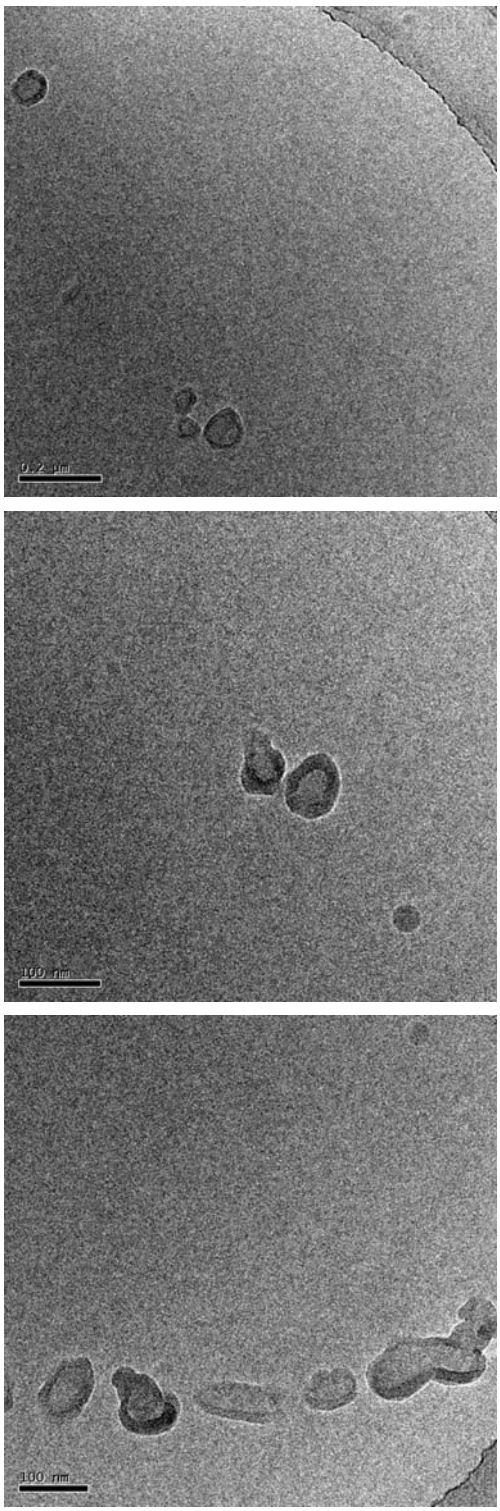

Figure S3: Several cryo-TEM pictures of the vesicles observed for the *tri*-arm star metallo supramolecular block copolymer.